CrystEngComm

Accepted Manuscript

This article can be cited before page numbers have been issued, to do this please use: K. K. Jha, S. Dutta, V. Kumar and P. Munshi, *CrystEngComm*, 2016, DOI: 10.1039/C6CE01501H.

ROYAL SOCIETY OF CHEMISTRY

www.rsc.org/crystengcomm

ROYAL SOCIETY OF CHEMISTRY View Article Online
DOI: 10.1039/C6CE01501H

Journal Name

ARTICLE

Isostructural Polymorphs: Qualitative Insights from Energy Frameworks

Received 00th January 20xx,
Accepted 00th January 20xx

DOI: 10.1039/x0xx00000x

www.rsc.org/

Kunal Kumar Jha,[a] Sanjay Dutta,[a] Vijay Kumar[b] and Parthapratim Munshi*[a]

Three isostructural polymorphs with two dimensional and three dimensional similarities are demonstrated quantitatively from similarity relationship analysis. The similarity dimensions are then visualized and correlated in a novel way *via* qualitative analysis using 'energy frameworks'. Two of the three polymorphs with three dimensional similarities exhibiting alike physical properties are having almost equi-energetic crystal structures while the most stable third polymorph exhibits distinct properties. Thereby structure-property correlations are derived, both quantitatively and qualitatively.

Introduction

Isostructurality and polymorphism, despite being two contradictory phenomena, exist together in crystal structures. While the occurrence of *similar* crystal structures of *different* compounds refers to isostructurality,[1] the phenomena of existence of at least two *different* crystal structures of a *same* compound refers to polymorphism.[2] Recently, Bernstein and his co-workers have reviewed the history of polymorphism phenomena and its facts and concluded upon systematic screening that the occurrence of polymorphs in molecular crystals is frequent.[3] Based on their database analysis and also experiments Fabian and Kalman have demonstrated the existence of isostructural polymorphs in molecular crystals and their similarity dimensions.[4] While one- and two-dimensional (1D and 2D, respectively) isostructurality[4c] in polymorphic systems has been discovered in several occasions,[5] three-dimensional (3D) similarities among polymorphs are rare.[6] Occasionally identifying very similar yet different structures as polymorphs might become difficult. In the context of borderline cases of similarity and dissimilarity in polymorphic structures, Desiraju questioned "when it is a matter of chemical common sense or quantitative crystallographic indicators, which criterion prevails?"[7] Both, concept of "supramolecular synthon",[8] which implies spatial arrangements of intermolecular interactions in crystals and "supramolecular construct",[9] which implies spatial arrangement of molecules in crystals, are used to identify the similarity among crystal structures and polymorphs. While the former can be identified from molecular packing analysis, the latter approach helps quantifying the similarity relationship between crystal structures. Energetics of polymorphs and especially of the isostructural ones are often nearly equal and characterizations of such structures warrants careful investigation.[10] While quantification of intermolecular interaction energies using Gavezzotti's PIXEL method[11] is quite popular, Spackman has recently introduced the concept of 'energy frameworks'[12] – a novel graphical representation of the magnitude of interaction energies. 'Energy frameworks', which provides qualitative picture of 3D-topology of the predominant interactions in molecular crystals, pertains to the various properties of crystals as well.

In this paper we present three polymorphs of (*Z*)-3-(3,4-dimethoxyphenyl)-2-(4-nitrophenyl)acrylonitrile (Scheme I), here after called ***m*-MeO-CMONS** – the *meta*-methoxy derivative of CMONS;[13] a well-known NLO material,[14] which also exists in polymorphic forms. Moreover, CMONS and its derivatives, similar to the one studied here, are known to serve as anti-cancer and anti-microbial agents.[15] In the present study, crystallization of freshly synthesized ***m*-MeO-CMONS** (See ESI) from its slow evaporation in various solvents often resulted in the original form (**P1**)[16] and on some occasions two more new forms (**P2** and **P3**) were discovered (Table S1, ESI). Interestingly, all three crystal forms exhibit distinct cell parameters belonging to the space group $P\bar{1}$ with two crystallographically independent molecules in the asymmetric unit, $Z' = 2$ (Table 1 and Fig. 1). This scenario is extremely rare and to the best of our knowledge there are only two more such cases reported in the Cambridge Structural Database;[17] Ref codes: MELFIT03/04/06 and SOBPEE/01/02. The former one, aripiprazole drug, exists in nine polymorphic forms and is the most polymorphic drug published to date. ***m*-MeO-CMONS** being the third one in this series and having biological importance of its analogs we have performed thorough

[a] *Chemical and Biological Crystallography Laboratory, Department of Chemistry, School of Natural Science, Shiv Nadar University, Tehsil Dadri, Uttar Pradesh-201314, India. E-mail: parthapratim.munshi@snu.edu.in*
[b] *Department of Chemistry, Central University of Gujarat, Gandhinagar, Gujarat-382030*

† Electronic Supplementary Information (ESI) available: Details of experimental and computational methods, Characterization techniques: single-crystal and powder X-ray diffraction, DSC, HSM, energy calculations. CCDC 1456630, CCDC 1456631 and CCDC 1456632. See DOI: 10.1039/x0xx00000x

characterizations of its polymorphs and correlated their properties with their respective structures, in a novel way.

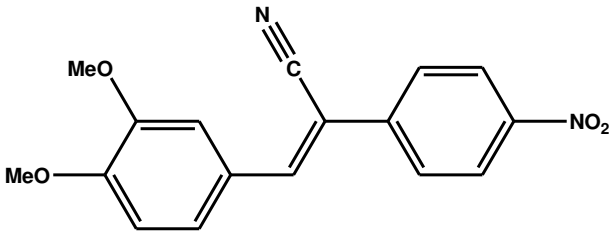

Scheme I: Chemical diagram of (*Z*)-3-(3,4-dimethoxyphenyl)-2-(4-nitrophenyl)acrylonitrile

Experimental Section

Synthesis

***m*-MeO-CMONS** [(*Z*)-3-(3,4-dimethoxy phenyl)-2-(4-nitrophenyl)acrylonitrile] was synthesized by condensation of 4-nitrophenylacetonitrile and 3,4-dimethoxybenzaldehyde in ethanol at 70°C for three hours in the presence of piperidine as basic catalyst as reported earlier (Scheme S1).[16]

Characterizations

Infrared spectra (FT-IR) of the solid samples were recorded on a Thermo Scientific *Nicolet iS5* spectrophotometer equipped with iD5-ATR accessory, in the range of 4000 – 400 cm^{-1}. Samples were prepared by crushing the respective crystal forms. 1 mg of sample was used to perform the experiment after taking into account of the background due to air media. ^1H NMR spectroscopy study was carried out using Bruker AVHDN 400 spectrometer. UV-Vis experiment was performed using Thermo Scientific Evolution 201 spectrophotometer. Samples were prepared by dissolving 1 mg of respective crystals in 10 ml of ethyl acetate. The clear solutions obtained were tested by UV-Vis spectroscopy. Powder X-ray diffraction (PXRD) patterns were recorded on a Rigaku Ultima IV diffractometer using Cu K_α radiation. The powder samples were prepared after grinding the respective polymorphic crystal forms. Differential scanning calorimetry (DSC) measurements on all three polymorphic crystals and also on bulk sample were carried out using Mettler Toledo DSC1 model under nitrogen gas (40 ml/min) atmosphere. Hot stage microscopy (HSM) studies on three crystal forms were carried out using Leica polarizing microscope MZ75 equipped with heating stage P350. Leica IM 50 software was used for image grabbing and monitoring the sample temperatures.

Crystallization

A range of HPLC grade solvents and their combinations at room temperature (22-25°C) and low temperature (3-6°C) were used for the crystallization of ***m*-MeO-CMONS** *via* slow evaporation method. The solvents, crystallization conditions and the outcome of the crystallization experiments are listed in Table S1. The crystal morphologies as captured using Olympus SZX10 Polarized Microscope equipped with digital camera are shown in Fig. S4.

Crystallography

View Article Online
DOI: 10.1039/C6CE01501H

Single crystal X-ray diffraction data were collected using D8 Venture IμS microfocus dual sources Bruker *APEX3* diffractometer equipped with PHOTON 100 CMOS detector and Oxford cryogenic system. Monochromatic Mo K_α radiation (λ=0.71073 Å) was used for the data collection using phi (ϕ) and omega (ω) scan strategy. All three data sets were collected at 100(2) K using exposure time per frame of 7s for **P1**, 17s for **P2** and 4s for **P3** and keeping the crystal to detector distance at 40mm. The cell measurement, data collection, integration, scaling and absorption correction was done using *APEX3* software.[18] The data was processed using *SAINT*[19] and an absorption correction was applied using *SADABS*[20] integrated in *APEX3*. The structure was solved using *SHELX*[21] program and refined using X*SHELL* program, both implemented in *APEX3*. Same strategy was adopted for solution and refinement of all three forms. The non-H atoms were located in successive difference Fourier syntheses and refined with anisotropic thermal parameters. All the hydrogen atoms were placed at calculated positions and refined using a riding model with appropriate HFIX commands. The program *Mercury*[22] was used for molecular packing analysis. The detailed crystallographic data has been summarized in Table 1.

Table 1 Single crystal X-ray diffraction data and the refinement parameters

Polymorphs	P1[16]	P2	P3
Formula	$C_{17}H_{14}N_2O_4$	$C_{17}H_{14}N_2O_4$	$C_{17}H_{14}N_2O_4$
Crystal size (mm)	0.089 x 0.177 x 0.183	0.052 x 0.151 x 0.218	0.102 x 0.260 x 0.397
Formula weight	310.30	310.30	310.30
Space group	$P\bar{1}$	$P\bar{1}$	$P\bar{1}$
a(Å)	10.2321(4)	8.6636(4)	7.6956(2)
b(Å)	11.9576(5)	11.9452(6)	12.3234(4)
c(Å)	12.2700(5)	14.3305(7)	15.6647(5)
α(°)	91.0010(10)	100.527(2)	82.0790(10)
β(°)	99.5610(10)	90.917(2)	86.3800(10)
γ(°)	100.1880(10)	95.640(2)	84.4590(10)
Volume ($Å^3$)	1455.36(10)	1450.15(12)	1462.66(8)
Z; *Z'*	4; 2	4; 2	4; 2
Density (g cm^{-3})	1.416	1.421	1.409
F(000)	648	648	648
μ (mm^{-1})	0.103	0.103	0.102
T_{min} ; T_{max}	0.913, 0.959	0.884, 0.986	0.923, 0.973
R(merge)	0.0428	0.0575	0.0518
Measured reflections	28719	38022	42858
Unique reflections	5536	5517	5556
No. of parameters	420	420	420
$R(F^2)$	0.0405	0.0628	0.0457
$R_w(F^2)$	0.0942	0.1390	0.1047
S	1.038	1.106	1.053
$\Delta\rho_{max}$ (e $Å^{-3}$)	0.28	0.62	0.48
$\Delta\rho_{min}$ (e $Å^{-3}$)	-0.21	-0.270	-0.24

Computational Section

Hirshfeld surface analysis

The package *CrystalExplorer 3.1*[23] was used to perform the Hirshfeld surface analysis on each of the symmetry independent molecules of all three forms. The analysis was carried out based on their respective crystal geometries. The corresponding 2D fingerprint plots were also generated using *CrystalExplorer 3.1*.

XPac analysis

The similarity relationship among the polymorphs and their dimension of similarity was analysed using the *XPac 2.0* program.[9] The crystal geometries of form **P1**, **P2** and **P3**, as obtained from single-crystal X-ray diffraction experiment were used for this purpose. Structure fragments were defined based on the best figure of merit and lowest filter.

Interaction energy calculation

CrystalExplorer 3.1 was used to evaluate the interaction energies of all three polymorphs. The energy components calculated within this procedure are electrostatic, polarization, dispersion and exchange-repulsion and finally the total interaction energy. These energy calculations are performed at the B97D3/6-31G(d,p) level of theory and using crystal geometries of the respective forms. All the hydrogen bond (HB) distances were set to the default value of 1.083Å. The scale factor was also set to the default value of 1.0.[24] The detailed computational procedure of these calculations has been discussed in ESI. Interaction energies were also calculated for all three polymorphs using the UNI force field.[25]

Energy frameworks analysis

Energy frameworks for all three polymorphs have been constructed based on the interaction energies as discussed above and the frameworks were visualized using the *CrystalExplorer 3.1*. The tube size (scale factor) used in all the energy frameworks was 10 and the energy threshold (cut off) value was set to zero.

Lattice energy calculations

The following two approaches were considered for the calculation of lattice energies of all three polymorphs.

PIXEL calculation

The intermolecular interaction energies in the crystal lattices were estimated by using *PIXEL* (version November 2015) program.[11] The molecular electron density required for this calculations were obtained by using *Gaussian09*[26] upon generating the input from *PIXEL*. The electron density calculations were performed at MP2/6-31G** level of theory and using their crystal geometries after setting the HB distances to 1.083Å, as used in *CrystalExplorer*. The densities were then used in PIXEL program to calculate the four energy terms; Coulomb, polarization, dispersion and repulsion. Thereby the lattice energies of each form were calculated.

Crystal14 calculation

Crystal14 program[27] was used to calculate lattice energy at the B97D/6-31G** level of theory and using crystal geometries after setting the HB distances to 1.083Å, as used above. Same scale factor of 1.0 as used for the calculations using *CrystalExplorer* is also used here. The dispersion factor was taken into account by inserting GRIMME keyword in the third block of input file, calculates a London-type pairwise empirical correction to the energy as proposed by Grimme.[28] The lattice energies were then calculated based on the following expression.

$$E_{latt} = E_{cryst}/Z - E_{mol}$$

Where E_{cryst} is the energy of the crystal, Z is the number of molecules in the unit cell and E_{mol} is the energy of a single molecule in the lattice.

The energy term E_{cryst} was calculated based on the periodic calculation on the crystal lattice and the term E_{mol} was obtained by performing calculation on two molecules extracted from the crystal lattice, as here in all three cases there are two molecules in the asymmetric unit.

Results and Discussion

Systematic crystallization experiment using various solvents resulted in two new polymorphic forms of compound ***m*-MeO-CMONS** (Table S1). The best diffraction quality crystals of form **P1** was grown from 1,4-dioxane at low temperature (4^0C). While both the forms **P2** and **P3** were grown from toluene, **P2** was achieved from crystallization at room temperature (RT) but **P3** at low temperature. Interestingly, crystal of from **P2** was achieved only from the crystallization using toluene at RT. However, all three polymorphic crystal forms are reproducible from the respective crystallization conditions as tabulated in Table S1. In most of the cases, at room temperature, crystals appeared overnight. However, for low temperature crystals were obtained in about 2-3 days.

X-ray diffraction experiments carried out on the best quality crystals revealed that all three crystal forms belonging to the space group $P\ \bar{1}$ exhibit $Z' = 2$ (Table 1). The structure has a stilbene like core with cyano (-CN) substitution on C=C bond having two phenyl ring at the two ends. One of the phenyl rings has acceptor nitro group (-NO_2) while the second phenyl ring has two donor methoxy groups (-MeO) at the *meta* and *para* position (Scheme I). The orientation of the two symmetry independent molecules in the asymmetric unit of the three forms represented with orange and green colour codes for molecules **A** and **B**, respectively, is depicted in Fig. 1. In each form the molecules **A** and **B** are aligned anti-parallel to each other forming a dimer *via* C-H…N interactions of varying geometry (Table 2). Overlay diagrams of the polymorphs suggest that the orientation of molecules **A** and **B** in form **P1** is distinct from those in forms **P2** but almost identical with **P3**. Distinct orientation of molecules **A** and **B** was also noticed between the forms **P2** and **P3** (Fig. S6, ESI). In all three forms the molecules **A** and **B** in the asymmetric unit exhibit similar conformations. Almost indistinguishable overlay diagram of

View Article Online
DOI: 10.1039/C6CE01501H

molecules **A** and **B** (Fig. S7, ESI), the marginal variations in torsion angles about the central C=C bond and the negligible angle between the overlaying planes (Table S2) clearly justify their conformational similarity.

Distinct molecular arrangements are noticed across the unit cells of the three polymorphic forms (Fig. 2). However, the orientation of molecules in form **P2** can somewhat be achieved by applying 2-fold rotational symmetry along *b*-axis to the molecules in form **P3**. Remarkably, almost identical undulating and layered molecular packing pattern is noticed across all three forms while viewed down the particular planes (Fig. 3). These similar packing patterns indicate that these polymorphs are isostructural. The presence of acceptor O-atoms in the nitro and methoxy groups and N-atom in cyano group along with the weak C(sp^2)-H donors forming weak intermolecular interaction directs the monolayer packing in all three forms. Weak C(sp^2)-H$\cdots\pi$ and H$\cdots$H interactions are also contributing to the stability of the crystal structure. 3D structures are further stabilized by the $\pi\cdots\pi$ interactions between the layers (Fig. S9). Moreover, the 2D layers formed *via* C-H$\cdots$N, C-H$\cdots$O and C-H$\cdots\pi$ interactions between the molecule **A** and molecule **B** and among themselves are remarkably similar for the forms **P1** and **P3** (Fig. 4). A slightly different interaction picture is noticed in form **P2**.

Table 2: Interaction geometry of C-H…N dimer

Forms	Distance (Å)		Angle (°)	
	H2···N2A	N2···H2A	∠C2-H2…N2A	∠C2A-H2A…N2
P1	2.693	2.457	126.36	132.50
P2	2.696	2.508	126.78	136.40
P3	2.667	2.533	123.04	129.37

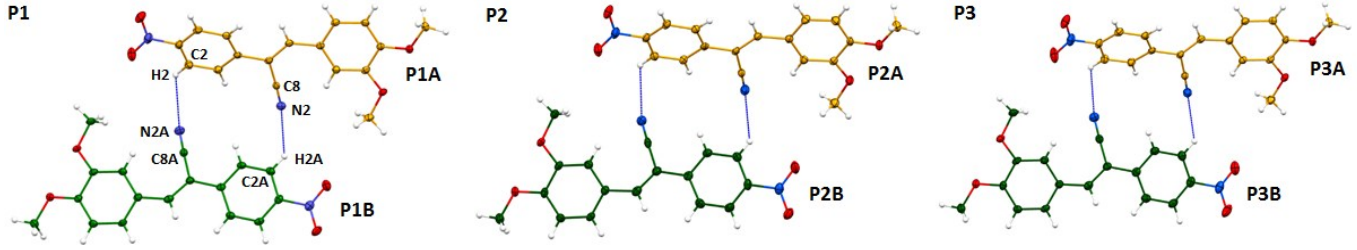

Fig 1 Ellipsoid plots of two symmetry independent molecules in the asymmetric unit drawn at 50% probability level for all three forms. H-atoms are drawn as fixed size spheres. Colour codes for different atom types as shown in form **P1** are same for forms **P2** and **P3**.

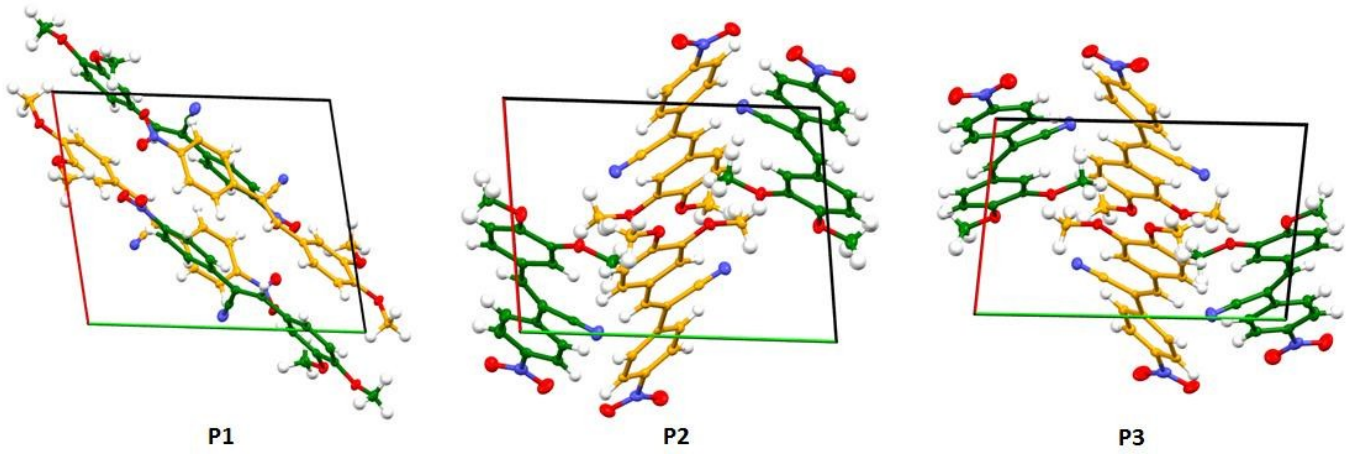

Fig. 2 Molecular packing in the unit cell of three forms viewed down the *c*-axis. The *a*-axis and *b*-axis is shown in red and green colors, respectively.

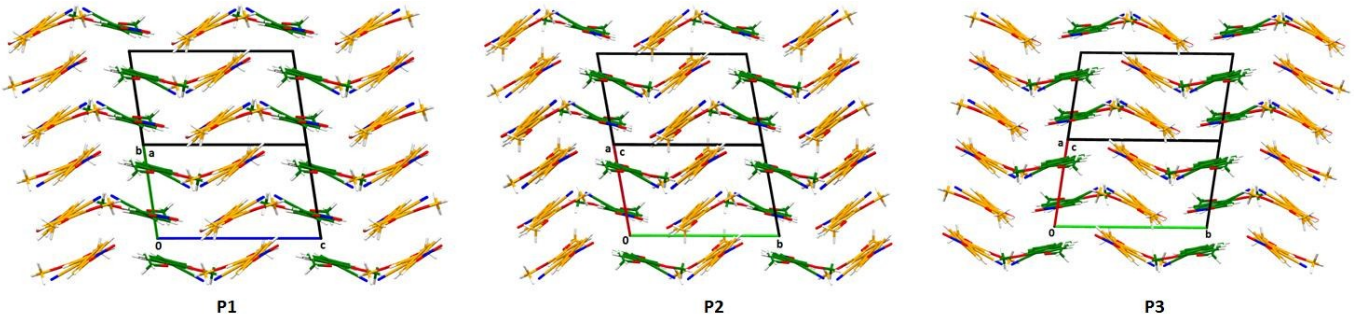

Fig. 3 Similarities in molecular packing diagram across the three polymorphs. Viewed down the (-1 1 0) for **P1** and (-1 0 1) for **P2** and **P3**.

View Article Online
DOI: 10.1039/C6CE01501H

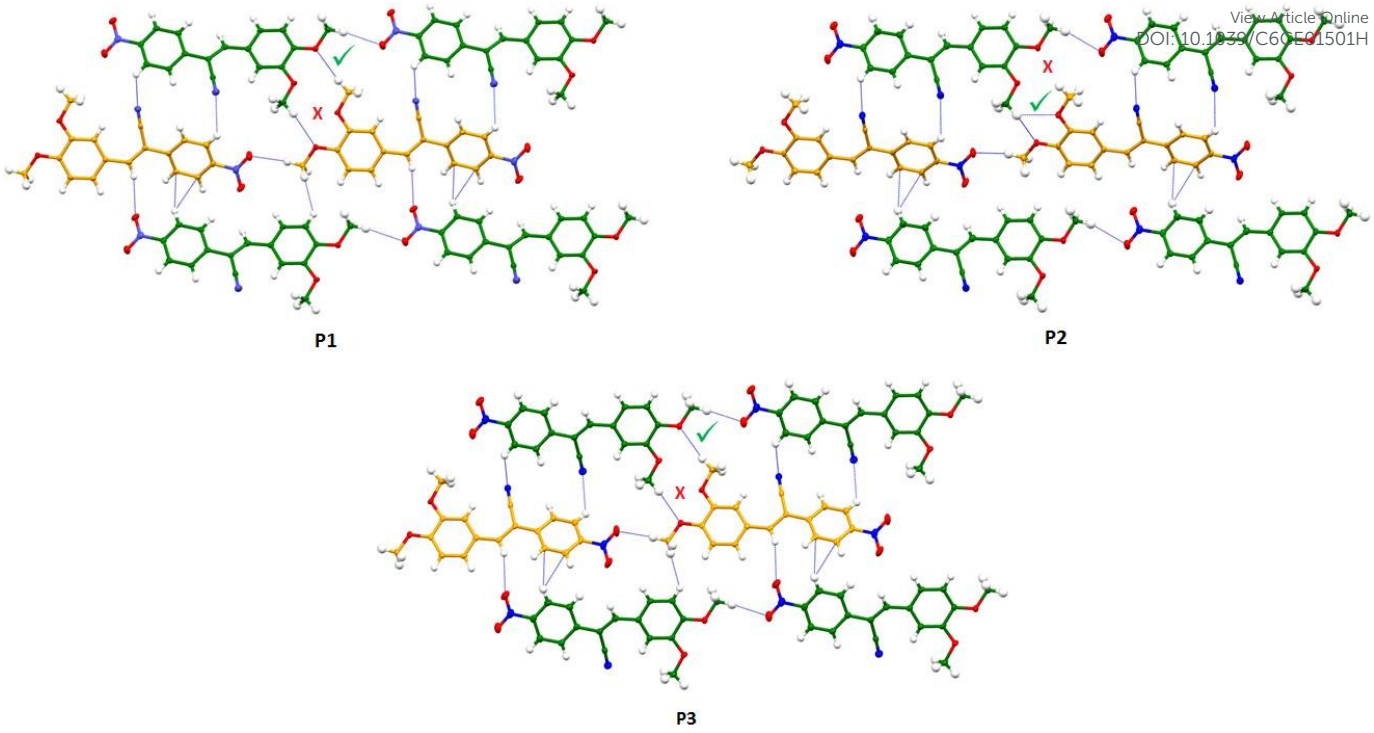

Fig. 4 Monolayer interaction motifs of forms **P1**, **P2** and **P3** showing the absence (X) and presence (✓) of intermolecular contacts

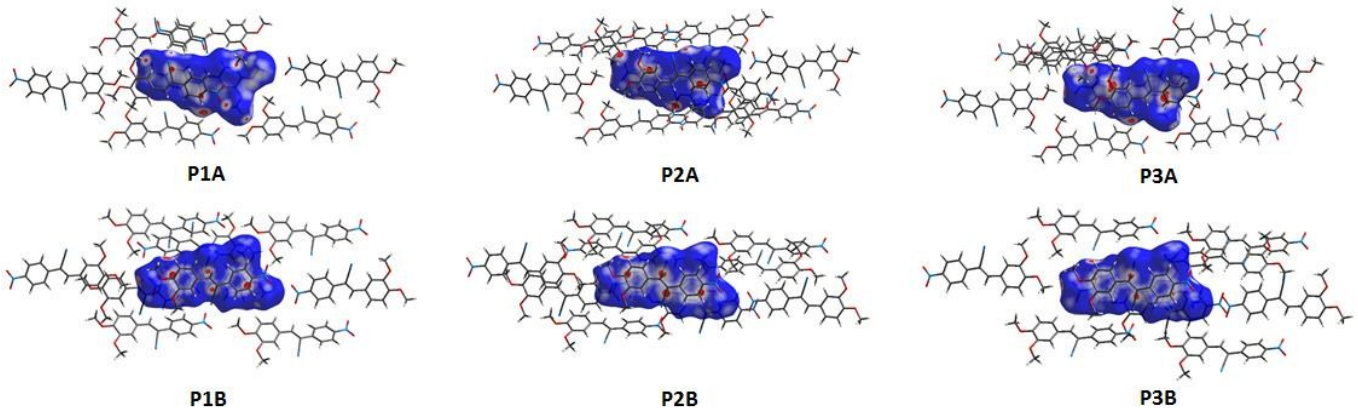

Fig 5 d_{norm} mapped on Hirshfeld surfaces of two independent molecules in the asymmetric unit of the three polymorphic forms

Further, in order to visualize and quantify the similarities and differences in intermolecular contacts across three polymorphs, we performed Hirshfeld surface analysis[29] based on their crystal geometries. The analysis was done individually for the molecules **A** and **B** present in the asymmetric unit of each form. The contact points as highlighted in the Hirshfeld surface of molecule **B** of each form clearly display the similarity of intermolecular interactions generated by molecule **B** of all three polymorphic forms (Fig. 5). Such similarities are also evident in the case of molecule **A** of forms **P2** and **P3**, whereas that of form **P1** exhibited slightly different intermolecular contacts. However, in each case the variation of strength of intermolecular interactions can be gauged from the changes in area of the red surfaces at the respective contact regions. Further, the similarities/dissimilarities of intermolecular contacts in different molecular environment of the three polymorphic forms are quantified *via* fingerprint plots[30] (Fig. S10**,** ESI) as generated from Hirshfeld surface analysis and the resulting histogram is depicted in Fig. 6. Hirshfeld surfaces and the associated fingerprint plots together help quantifying intermolecular contacts, conveniently. Shortest O···H contacts are noticed for molecule **A** of form **P1**, labelled with purple triangle in the fingerprint plot (Fig. S10**,** ESI). The subtle variations in fingerprint plots for all the six molecules highlight the differences in the crystal environment across the three polymorphic forms. The comparison as depicted in Fig. 6 reveals that for all the six molecules O···H hydrogen bonding and H···H interactions together are associated with nearly 58% of the surface area. Moreover, the histogram reflects the striking similarities of percentage contributions to the Hirshfeld surface area for the various close intermolecular contacts of molecule **B** of all three forms and also for molecule

A of the forms **P2** and **P3**, with slight variation of O···H contacts (27% *vs* 30%) for **P1A.**

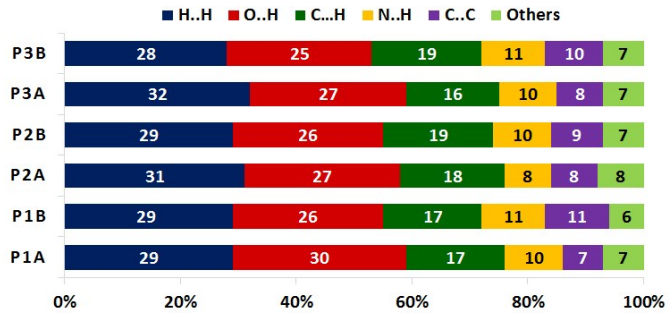

Fig. 6 Percentage contributions to the Hirshfeld surface area for the various close intermolecular contacts in molecules **A** and **B** of the three polymorphic forms.

Table 2 Comparison of the categorization of the degree of isostructurality among the three polymorphic forms, obtained using XPac analysis.

Polymorphs	**P1 vs P2**	**P1 vs P3**	**P2 vs P3**
Dimensionality	2D	2D	3D
Dissimilarity Index (X)	7.3	3.8	7.6
Stretch Parameter (D)	0.15	0.04	0.27
Δa (angles, deg)	2.0	0.8	2.8
Δp (planes, deg)	6.9	3.7	6.9

Further, XPac[9] analysis was performed to quantify the similarity relationship among these three polymorphic crystal structures. While such similarities are traditionally interpreted for whole 3D structures, it is also extended for 2D molecular layers of the crystal structures.[6] The results from XPac analysis are listed in Table 2. The relevant plots from XPac analysis as obtained from the program are given in ESI. The values of the different parameters obtained by comparison among three polymorphs are well within the isostructurality limits as discussed by Coles *et al.* The comparison clearly suggests that form **P1** is two dimensionally similar to the forms **P2** and **P3** and the highest degree of isostructurality is noticed between the forms **P1** and **P3**. This supports the striking similarity of the interaction motifs between the forms **P1** and **P3** when examined in a layer, as discussed above (Fig. 4). Further, the XPac analysis reveals that there is a 3D similarity between the polymorphs **P2** and **P3**, which has also been realized from the comparison of structural conformations, 3D molecular packing and intermolecular contact analysis, demonstrated above. Although such analysis provides a quantitative measure of the similarities among the crystal structures it fails to deliver a qualitative picture.

Furthermore, the actuality of isostructurality among these polymorphic forms is qualitatively validated in a novel way *via* 'energy frameworks',[12] constructed using CrystalExplorer.[23] The values of interaction energy calculated between the molecular pairs in each crystal form (Table S3 – S5, ESI) are used to frame the 3D-topology of major interactions and thereby the energy frameworks are constructed. A systematic comparison of the total energy frameworks across three isostructural polymorphs reveals that forms **P2** and **P3** are remarkably similar and that of form **P1** is also somewhat

View Article Online
DOI: 10.1039/C6CE01501H

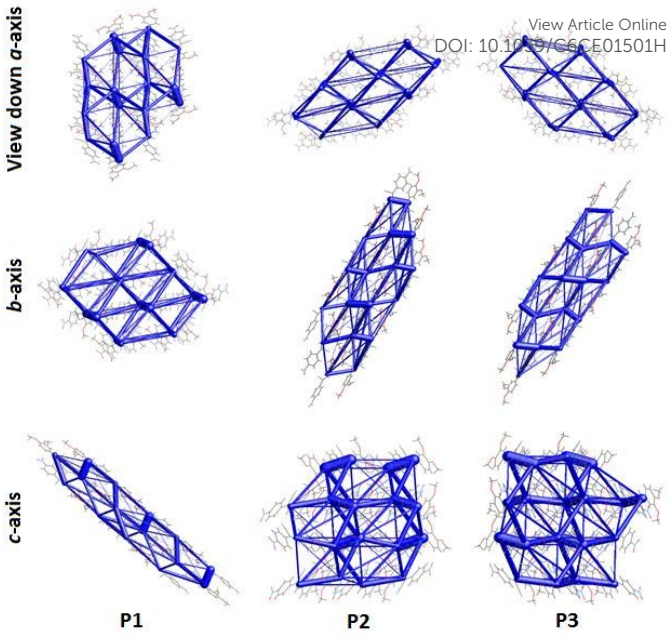

Fig 7 Energy frameworks corresponding to the total interaction energy in all three polymorphs with 10 energy scale factor and zero energy threshold. The figures are on the same spatial scale

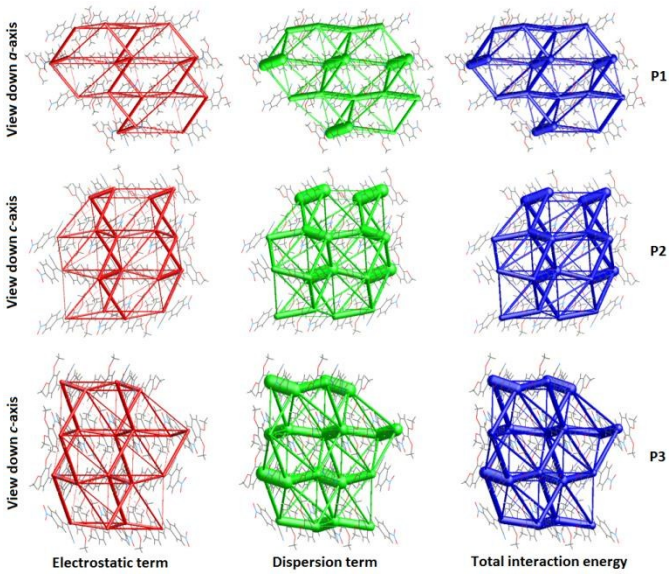

Fig. 8 Energy frameworks corresponding to the different energy components and total interaction energy in **P1**, **P2** and **P3**

similar (Fig. 7). However, a slight variation in the dimension of the pillars, crossbars and columns between the forms **P2** and **P3** is noticed. In the case of form **P1**, the views down the *b*-axis and *c*-axis look similar to the views down the *a*-axis and *b*-axis of forms **P2** and **P3**, respectively. However, form **P1** is found to show less similarity with forms **P2** and **P3**, along the third direction. Energy frameworks of form **P1** appeared to have slightly higher degree of similarity with that of form **P3** than form **P2**. Similarity in electrostatic and dispersion energy-frameworks, with dispersion energy being the dominating term, was also noticed among all three polymorphs (Fig. 8,

Figs. S14 – S16, ESI). Indeed, these qualitative pictures of energy frameworks strongly correlate with the dimensionalities and dissimilarity indices as estimated from XPac analysis (Table 2). Striking similarities of energy-frameworks are also noticed in the case of 3D isostructural polymorphs of 3-chloromandelic acid[6] (Fig. S17 – S19, ESI) and rather surprisingly, in the case of so-called 'quasi-isostructural polymorphs'.[31]

The molecular pair-wise interaction energies calculated for the construction of energy frameworks are used to evaluate the net interaction energies in each form. A shell of nearest neighbouring molecules around each symmetry independent molecule, termed residue, is considered for this calculation (Figs. S11 – S13, ESI). The average neighbouring-shell net interaction energy values (Table S6) for form **P1**, **P2** and **P3** are -230.6 kJ mol^{-1}, -221.6 kJ mol^{-1} and -225.4 kJ mol^{-1}, respectively. A similar trend is noticed when energies for the intermolecular potential were calculated using the UNI force field (Table S7).[25] Not surprisingly, the interaction energy values of these isostructural polymorphs are fairly comparable. The computation of packing energies[25] provided the values of -179.7 kJ mol^{-1}, -178.0 kJ mol^{-1} and -175.8 kJ mol^{-1} for forms **P1**, **P2** and **P3**, respectively. Likewise, the lattice energies calculated using *PIXEL* code[32] indicates (Table S8) that form **P1** is the most stable form (-147.3 kJ mol^{-1}) followed by form **P2** (-143.6 kJ mol^{-1}) and form **P3** (-143.0 kJ mol^{-1}). Lattice energies calculated using *Crystal14*[27] program (Table S9) also show a similar trend; -231.3 kJ mol^{-1} for **P1**, -229.1 kJ mol^{-1} for **P2** and -228.3 kJ mol^{-1} for **P3**. Interestingly, the 3D isostructural polymorphs **P2** and **P3** are almost equi-energetic and the form **P1**, which has 2D similarity with the former forms, appear to be the energetically most stable form. Therefore, form **P1** appears in almost all of the crystallization attempts than the other forms.

For all three polymorphic forms and also the bulk sample, the phase and enthalpy changes were monitored *via* DSC. The samples were heated at 2°C/min from 25°C to 250°C and cooled back to 30°C and the cycle repeated again for a second time. The phase and enthalpy changes occurred in the two successive heating cycles have been tabulated in Table S10. The bulk sample as well as all three forms showed similar trend of phase transitions (Fig. 9). In the first heating cycle, two phase changes appeared in all the samples; one small exothermic hump and another endothermic melting peak. While cooling, a single sharp exothermic peak is noticed except for form **P1**, in which a broad peak is noticed and so is the case during second cooling. In the second heating cycle, three phase changes are noticed; one exothermic peak and two endothermic peaks. DSC trace of bulk sample looked similar to that of forms **P2** and **P3**. Further, these phase changes are visualized *via* HSM (Fig. S20). In all three forms a crystalline new phase appeared at around 165°C - 185°C, which may correspond to the exothermic peak appeared in the DSC traces around 152°C - 156°C, and finally melted at around 208°C - 220°C. Similar trend in melting point is noticed in their DSC traces; form **P1** has slightly lower melting point (178.1^{0}C) than forms **P2** (179.5^{0}C) and **P3** (179.4^{0}C), as recorded from the respective peak maximum. The needle shaped crystals appeared between 165°C - 185°C for each of the crystal forms as seen in the HSM images are further examined under the X-ray. The cell check experiment revealed that this is yet another crystal form with new cell parameters and belongs to once again in triclinic crystal system.[33] Unfortunately, the structure of this new form couldn't be solved as these crystals diffracted poorly even at low temperature and using Microfocus X-ray sources (*Mo* and *Cu*). Form **P1** is seen to form glassy (amorphous) materials during cooling at around 140°C, which corresponds to the glass transition peak in DSC at around 105°C - 125°C. Forms **P2** and **P3** are found to behave similarly during the cooling cycle. A semi opaque material is noticed at around 90°C for form **P2**, which seems to be corresponding to the exothermic peak at around 132°C in the DSC trace and at around 80°C for form **P3**, which seems to be corresponding to the exothermic peak at around 123°C in the DSC trace. The thermal stabilities of the polymorphs as investigated *via* DSC and HSM measurements once again suggested that form **P1** is slightly different from the 3D isostructural forms **P2** and **P3**. The slight higher melting point for forms **P2** and **P3** may be due to the existence of some stronger pillars (greater intermolecular forces) in their energy frameworks than in **P1** (Figs. 7 & 8).

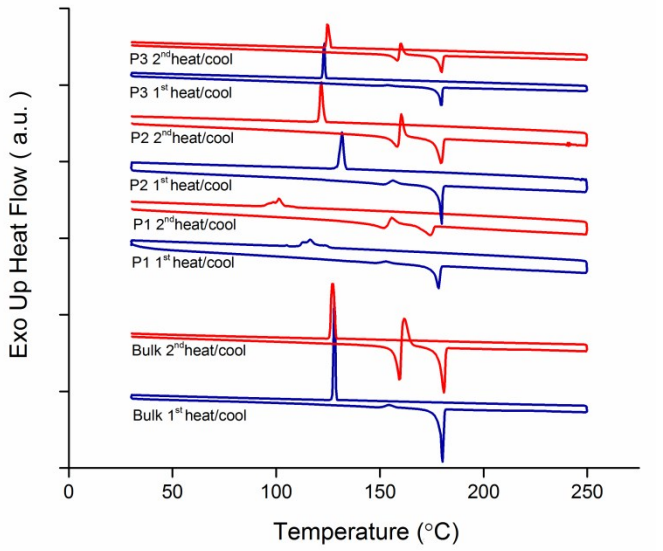

Fig. 9 Traces of DSC for the bulk sample and polymorphs **P1**, **P2** and **P3**.

The polymorphs were further characterized using PXRD. The scan rate used for these measurements is 1°/min with 0.02° step in 2θ. The experimental PXRD patterns of forms **P1**, **P2** and **P3** recorded at room temperature were then compared with their corresponding simulated PXRD patterns generated from the respective single-crystal structures of forms **P1**, **P2** and **P3** (Fig. 10) also determined at room temperature.[34] The comparison displaying reasonably good agreement between the observed and predicted patterns justifies the phase purity of the polymorphic forms. However, for form **P2,** at around 15° in 2θ, the predicted pattern shows two peaks whereas the observed pattern shows only one peak, which seems to be the

average of the two predicted peaks. The similar marginal shifts and discrepancies between the simulated and observed PXRD pattern are also noticed in a recent study on 'quasi-isostructural polymorphs'.[31] Observed PXRD patterns of the three forms are also compared (Figure S20) to highlight the subtle differences of the phases of these isostructural polymorphic forms. While variable temperature PXRD studies on these polymorphs could be useful to probe the effects of heating and cooling and to check for any thermally-induced phase transitions the quantitative DSC traces and the qualitative HSM images as highlighted above certainly serve these purposes.

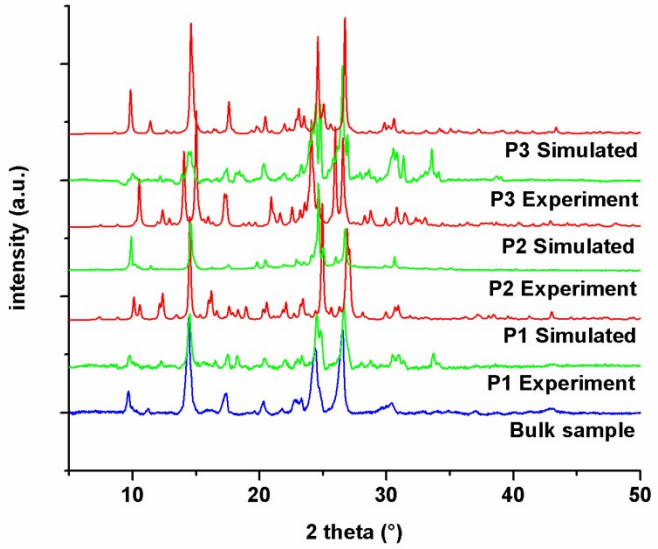

Fig. 10 Experimental and simulated PXRD patterns of forms **P1**, **P2** and **P3** along with bulk sample

Being isostructural polymorphs the FT-IR spectra of each form exhibited identical features (Fig. S1, ESI). Also UV-Vis spectra of all three polymorphic forms showing λ_{max} value of 384.17 nm (Fig. S2, ESI) fall into the category of 'yellow material',[35] which find tremendous applications in dye industries.[36]

Conclusions

In summary, unusual polymorphic forms of *m*-MeO-CMONS with all three having $Z' = 2$ and space group $P\bar{1}$ are discovered to exist as isostructural. Systematic quantitative and qualitative analyses based on the supramolecular constructs and the energy frameworks, respectively, revealed their degree of similarity and dimensions. Thereby structure-property correlations were derived directly through the graphical representation of the meaningful energy frameworks. Similarity/dissimilarity of physical properties among the polymorphs is well correlated with their respective similarity dimensions. This novel way of studying polymorphs, especially the tricky isostructural ones, may expand the scope of research in crystal engineering and instigate pharmaceutical industries to perform such analysis systematically yet rapidly.

Acknowledgment

View Article Online
DOI: 10.1039/C6CE01501H

We thank Shiv Nadar University for research facilities, infrastructure and funding and also research fellowship to KKJ and SD. We are grateful to Prof. Rupamanjari Ghosh for her kind encouragements and supports. Thanks to Prof. M. A. Spackman and Prof. D. Jayatilaka for the access to CrystalExplorer (energy framework analysis). We thank Dr. R. G. Gonnade for HSM images and Dr. A. Roychoudhury for certain helps. We are thankful to one of the referees for providing valuable suggestions to improve this manuscript.

Notes and references

1 A. Kalman, S. Parkanyi and G. Argay, *Acta Crystallogr.*, 1993, **B49**, 1039.
2 W. C. McCrone, Physics and chemistry of the organic solid state, ed. D. Fox, M. M. Labes and A. Weissberger, *Wiley Interscience, New York, USA*, 1965, vol. 2.
3 A. J. Cruz-Cabeza, S. M. Reutzel-Edens and J. Bernstein, *Chem. Soc. Rev.*, 2015, **44**, 8619.
4 (a) L. Fabian and A. Kalman, *Acta Crystallogr.*, 1999, **B55**, 1099. (b) L. Fabian, A. Kalman, G. Argay, G. Bernath and Z. S. Gyarmati, *Chem. Commun.*, 2004, 2114. (c) L. Fabian and A. Kalman, *Acta Crystallogr.*, 2004, **B60**, 547.
5 (a) N. Zencirci, T. Gelbrich, V. Kahlenberg and U. J. Griesser, *Cryst. Growth Des.*, 2009, **9**, 3444. (b) M. B. Hursthouse, L. S. Huth and T. L. Threlfall, *Org. Process Res. Dev.*, 2009, **13**, 1231.
6 S. J. Coles, T. Threlfall and G. Tizzard, *Cryst. Growth Des.*, 2014, **14**, 1623.
7 G. R. Desiraju, *Cryst. Growth Des.*, 2008, **8**, 3.
8 G. R. Desiraju, *Angew. Chem. Int. Ed. Engl.*, 1995, **31**, 2311.
9 T. Gelbrich and M. B. Hursthouse, *CrystEngComm.*, 2005, **7**(53), 324.
10 G. R. Desiraju, *Science*, 1997, **278**, 404.
11 A. Gavezzotti, *Z. Krist.*, 2005, **220**, 499.
12 M. J. Turner, S. P. Thomas, M. W. Shi, D. Jayatilaka and M. A. Spackman, *Chem. Commun.*, 2015, **51**, 3735.
13 R. M. Vrcelj, E. E. A. Shephered, C. S. Yoon, J. N. Sherwood and A. R. Kennedy, *Cryst. Growth Des.*, 2002, **2**, 609.
14 H. S. Nalwa and S. Miyata, Nonlinear Optics of Organic Molecules and Polymers, *CRC Press*, 1996.
15 M. S. Alam, Y. Nam, D. Lee, *Eur. J. Med. Chem.*, 2013, **69**, 790.
16 A. M. Asiri, S. A. Khan, K. W. Tan and S. W. Ng, *Acta Crystallogr.*, 2010, **E66**, o1733.
17 F. H. Allen, *Acta Crystallogr.*, 2002, **B58**, 380.
18 Bruker *APEX* 3, Version 2, User Manual S86 –EXS053. Bruker AXS Inc, Madison, Wisconsin, USA, 2015.
19 Siemens, SMART system, Siemens Analytical X-ray Instruments Inc. Madison, MI, 1995.
20 G. M, Sheldrick , SADABS, Bruker AXS Inc, Madison, WI, 2007.
21 G. M, Sheldrick , *Acta Cryst*. 2008, **A64**, 112.
22 C. F. Macrae, P. R. Edgington, P. McCabe, E. Pidcock, G. P. Shields, R. Taylor, M. Towler and J. van de Streek, *J. Appl. Cryst.*, 2006, **39**, 453.
23 S. K. Wolff, D. J. Grimwood, J. J. McKinnon, D. Jayatilaka and M. A. Spackman, *Crystal Explorer;* University of Western: Perth, Australia, 2007; http://hirshfeldsurface.net/CrystalExplorer.
24 M. J. Turner, S. Grabowsky, D. Jayatilaka and M. A. Spackman, *J. Phys. Chem. Lett.*, 2014, **5**, 4249.
25 (a) A. Gavezzotti, *Acc. Chem. Res.*, 1994, **27**, 309. (b) A. Gavezzotti and G. Filippini, *J. Phys. Chem.*, 1994, **98**(18), 4831
26 Gaussian 09, Revision **E.01**, M. J. Frisch, G. W. Trucks, H. B. Schlegel, G. E. Scuseria, M. A. Robb, J. R. Cheeseman, G. Scalmani, V. Barone, B. Mennucci, G. A. Petersson, H. Nakatsuji, M. Caricato, X. Li, H. P. Hratchian, A. F. Izmaylov, J. Bloino, G. Zheng, J. L. Sonnenberg, M. Hada, M. Ehara, K. Toyota, R. Fukuda, J. Hasegawa, M. Ishida, T. Nakajima, Y. Honda, O. Kitao, H. Nakai, T. Vreven, J. A. Montgomery, Jr., J. E. Peralta, F. Ogliaro, M. Bearpark, J. J. Heyd, E. Brothers, K. N. Kudin, V. N. Staroverov, R. Kobayashi, J. Normand, K. Raghavachari, A. Rendell, J. C. Burant, S. S. Iyengar, J. Tomasi, M. Cossi, N. Rega, J. M. Millam, M. Klene, J. E. Knox, J. B. Cross, V. Bakken, C. Adamo, J. Jaramillo, R. Gomperts, R. E.

View Article Online
DOI: 10.1039/C6CE01501H

Stratmann, O. Yazyev, A. J. Austin, R. Cammi, C. Pomelli, J. W. Ochterski, R. L. Martin, K. Morokuma, V. G. Zakrzewski, G. A. Voth, P. Salvador, J. J. Dannenberg, S. Dapprich, A. D. Daniels, Ö. Farkas, J. B. Foresman, J. V. Ortiz, J. Cioslowski, and D. J. Fox, Gaussian, Inc., Wallingford CT, 2009.

27 R. Dovesi, R. Orlando, A. Erba, C. M. Zicovich-Wilson, B. Civalleri, S. Casassa, L. Maschio, M. Ferrabone, M. De la Pierre, P. D'Arco, Y. Noel, M. Causa, M. Rerat and B. Kirtman, *Int. J. Quantum Chem*, 2014, **114**, 1287.

28 S. Grimme. *J. Comput. Chem.*, 2006, **27**, 1787.

29 M. A. Spackman and D. Jayatilaka, *CrystEngComm*, 2009, **11**, 19.

30 J. J. Mckinnon, Jayatilaka and Spackman, *Chem. Commun*., 2007, 3814.

31 D. Dey, S. P. Thomas, M. A. Spackman and D. Chopra, *Chem. Commun*., 2016, **52**, 2141.

32 J. D. Dunitz and A. Gavezzotti, *Cryst. Growth Des*., 2012, **12**, 5873.

33 Cell parameters of the needle shaped crystals as obtained from HSM: a = 3.92 (15) Å, b = 19.10 (18) Å, c = 21. 04 (8) Å, α = 71.5 (7)°, β = 85.0 (2)° and γ = 89.8 (2)°, , V= 1490.00(30) Å^3.

34 Cell parameters using single-crystal X-ray diffraction data collected at room temperature; **P1**: a = 10.3185 (5) Å, b = 12.0948 (6) Å, c = 12.4088 (6) Å, α = 91.276 (2)°, β = 99.834 (2)°, γ = 98.874 (2)° , V= 1505.72(13) Å^3; **P2**: a = 8.7385 (5) Å, b= 12.0819 (7) Å, c = 14.5627 (8) Å, α = 79.608 (3)°, β = 89.477 (3)°, γ = 83.819 (3) °, V= 1503.40(15) Å^3; **P3**: a = 7.9476 (6) Å, b = 12.3304 (8) Å, c = 15.7276 (11) Å, α = 81.618 (3)°, β = 85.114 (3)°, γ = 83.978 (3)°, V= 1512.55(18) Å^3.

35 (a) J. Zyss, Conjugated Polymeric Materials: Opportunities in Electronics, Optoelectronics, and Molecular Electronics, J. L. Brédas and R. R. Chance (Eds.), *Kluwer Academic Publishers*, pp 545 – 557, 1990. (b) D. S. Chemla and J. Zyss, Nonlinear Optical Properties of Organic Molecules and Crystals, vol **1**, *Academic Press Inc.* 1987.

36 A. M. Asiri, *Dyes and Pigments*, 1999, **42**, 209.